

REVIEW

Open Access



# A review of novel methods to assist digital planning and execution of osteotomy for upper limb deformities

Yoshii Yuichi<sup>1\*</sup>, Sho Kohyama<sup>2</sup>, Akira Ikumi<sup>3</sup>, Yohei Yanagisawa<sup>3</sup>, Takushi Nakatani<sup>4</sup>, Junichiro Morita<sup>5</sup> and Takeshi Ogawa<sup>5</sup>

\*Correspondence:  
yyoshii@tokyo-med.ac.jp

<sup>1</sup> Department of Orthopaedic Surgery, Tokyo Medical University Ibaraki Medical Center, 3-20-1 Chuo, Inashiki, Ami, Ibaraki 300-0395, Japan

<sup>2</sup> Department of Orthopaedic Surgery, Kikkoman General Hospital, Noda, Chiba 278-0005, Japan

<sup>3</sup> Department of Orthopaedic Surgery, University of Tsukuba Hospital, Tsukuba, Ibaraki 305-8576, Japan

<sup>4</sup> Department of Orthopedic Surgery, Showa General Hospital, Kodaira, Tokyo, Japan

<sup>5</sup> Department of Orthopaedic Surgery, NHO Mito Medical Center Hospital, Ibaraki, Ibaraki 311-3193, Japan

## Abstract

Corrective osteotomy for upper limb deformities caused by fractures, trauma, or degeneration necessitates detailed preoperative planning to ensure accurate anatomical alignment, restore limb length, and correct angular deformities. This review evaluates the effectiveness of a three-dimensional (3D) preoperative planning program and an image fusion system designed for intraoperative guidance during corrective osteotomy procedures. The application processes and clinical outcomes observed with these technologies in various surgical scenarios involving the upper extremities were summarized. The systems proved beneficial in allowing surgeons to visualize surgical steps and optimize implant placement. However, despite these technological advancements, we found no significant impact on clinical outcomes compared to conventional methods. This indicates a need for further enhancements in system efficiency and user-friendliness to significantly improve patient results. Future developments should focus on addressing these limitations to enhance the practical utility of such advanced systems.

**Keywords:** Corrective osteotomy, Malunion, Preoperative planning, Surgical simulation, Image fusion system, 3D visualization, Surgical navigation

## Background

The upper extremity is an organ responsible for functions essential for human social activities. The upper extremity function plays a central role in the ability to grasp/manipulate objects and fine movements that are important for activities, such as eating, changing clothes, and writing. When a deformity of the upper limb occurs due to fracture, trauma, or degeneration, functional recovery through accurate anatomical reconstruction is required. The deformities of the upper limb significantly impair functional capabilities. Corrective osteotomy poses a challenging issue in upper extremity surgical interventions aimed at addressing these deformities. Reconstruction of an alignment along three-dimensional axes, normal-length recovery, and correction of angular deformation are complex issues for orthopedic surgeons. A close



preoperative plan and measures to conduct corrective osteotomy in the operating room are necessary.

This review aimed to assess the clinical significance of 3D preoperative planning and the image fusion system and provide an overview of recent literature on computer-assisted techniques for corrective osteotomy of upper extremities over the past decade. In the first part in each section of this article, we introduce the application and clinical significance of a three-dimensional (3D) preoperative planning program for corrective osteotomy of the upper extremities and usefulness of the image fusion system which we developed for intraoperative assistance to precisely conduct the preoperative planning during the surgery. In the second part of each section, we reviewed the current computer-assisted technologies that orthopedic surgeons can use for the corrective osteotomy of the upper limb.

### Literature search methods and overall structure

We have done a PubMed search in April 2024 using the keywords “orthopedics”, “corrective osteotomy” and “computer assist”, as well as “orthopedics”, “corrective osteotomy” and “patient specific instrument” from 2014 to 2024. Each search yielded 162 and 116 results. According to the PRISMA flow diagram [1], we excluded those targeting areas other than upper extremities ( $n = 124, 91$ , respectively), case reports ( $n = 5, 2$ , respectively) non-English literature ( $n = 1, 1$ , respectively), and duplicated searched literature ( $n = 16$ ), ended up with 22 literatures (Fig. 1). For these literatures, two raters (Y.Y. and S.K.) independently assessed the quality of the studies according to the GRADE criteria (Table 1) [2]. After the independent evaluations, the raters discussed the discrepancies in their ratings and unified their ratings. The studies that met the criteria of low or higher were included. This review outlines the authors’ developments, the current knowledge and practice in the field of computer-assisted technology in corrective osteotomy of the upper extremity, and discusses future perspectives.

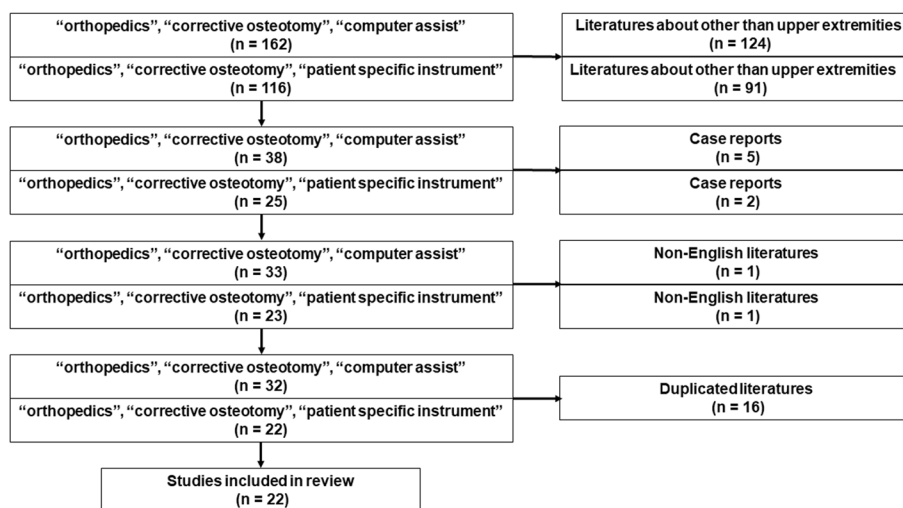


**Fig. 1** Flow diagram of included and excluded literatures

**Table 1** List of included literatures

Ref Nos.	Authors	Study design	Intervention	No. of participants	Disorders	Published Year	Evaluation
[18]	Prommersgerger et al	Case series	Conventional	49	Distal radius fracture, distal radius malunion	2002	Low
[19]	Schweizer et al	Case series	3D computer-based planning with patient-specific guides	6	Distal radius malunion	2013	Low
[20]	Murase et al	Case series	3D computer-based planning with patient-specific guides	22	Cubitus varus, forearm malunion, distal radius malunion	2008	Low
[21]	Vlachopoulos et al	Case series	3D computer-based planning with patient-specific guides	14	Extra-articular deformity of the forearm	2015	Low
[22]	Schweizer et al	Case control study	3D computer-based planning with or without patient-specific guides	22	Scaphoid nonunions	2016	Moderate
[23]	Roner et al	Case control study	3D computer-based planning with patient-specific guides	15	Distal radius malunion	2018	Moderate
[24]	Shintani et al	Case series	3D computer-based planning	19	Distal radius malunion	2018	Low
[25]	Stirling et al	Case series	Conventional	89	Distal radius malunion	2020	Moderate
[26]	Batra et al	Case series	Conventional	69	Distal radius fracture	2002	Moderate
[27]	Ali et al	Case series	Conventional	85	Distal radius malunion	2018	Moderate
[28]	Bujize et al	Randomized clinical trial	3D computer-based planning with patient-specific guides	40	Distal radius malunion	2018	Moderate
[32]	Singh et al	Case series	3D computer-based planning with patient-specific guides	6	Malunions of the forearm, radiocarpal, trapezio-metacarpal, and proximal interphalangeal joints	2020	Low
[33]	Kabelitz et al	Case series	3D computer-based planning with patient-specific guides	10	Phalanx malunion	2022	Low

**Table 1** (continued)

Ref Nos.	Authors	Study design	Intervention	No. of participants	Disorders	Published Year	Evaluation
[48]	Takeyasu et al	Case series	3D computer-based planning with patient-specific guides	30	Distal humerus malunion	2013	Low
[51]	Barbier et al	Case series	3D computer-based planning with patient-specific guides	5	Distal humerus malunion	2019	Low
[52]	Bauer et al	Case control study	3D computer-based planning with patient-specific guides	56	Malunions of the forearm	2017	Moderate
[53]	Zhang et al	Case control study	3D computer-based planning with patient-specific guides	25	Distal humerus malunion	2019	Moderate
[54]	Jin et al	Case control study	3D computer-based planning with patient-specific guides	40	Cubitus varus	2022	Moderate
[55]	Hu et al	Case control study	3D computer-based planning with patient-specific guides	35	Cubitus varus	2020	Moderate
[56]	Vlachopoulos et al	Surgical technique	3D computer-based planning with patient-specific guides	N/A	Proximal and distal humerus malunion	2016	Low
[57]	Oura et al	Case series	3D computer-based planning with patient-specific guides	2	Distal humerus malunion	2018	Low
[58]	Xue et al	Case series	3D computer-based planning	17	Elbow deformities	2023	Low

Study design	Journal	Published Year	Evaluation	
			Rator A	Rator B
Case series	J Hand Surg Br	2002	Low	Low
Case series	J Hand Surg Am	2013	Low	Low
Case series	J Bone Joint Surg Am	2008	Low	Low
Case series	BMC muskuloskelet Disord	2015	Low	Low
Case control study	J Hand Surg Am	2016	Low	Low
Case control study	BMC Musculoskeletal Disorders	2018	Low	Low
Case series	J Hand Surg Asian Pac	2018	Low	Low
Case series	Bone Joint J	2020	Moderate	Moderate
Case series	Injury	2002	Moderate	Moderate
Case series	J Bone Joint Surg Am	2018	Moderate	Moderate
Randomized clinical trial	J Bone Joint Surg Am	2018	Moderate	Moderate

**Table 1** (continued)

Study design	Journal	Published Year	Evaluation	
			Rator A	Rator B
Case series	Hand Surg Rehabil	2020	Low	Low
Case series	BMC Musculoskelet Disord	2022	Low	Low
Case series	J Bone Joint Surg Am	2013	Low	Low
Case series	Acta Orthop Belg	2019	Low	Low
Case control study	J Hand Surg Am	2017	Moderate	Moderate
Case control study	J Orthop Surg Res	2019	Moderate	Moderate
Case control study	Scientific Reports	2022	Moderate	Moderate
Case control study	J Orthop Surg Res	2020	Moderate	Moderate
Technical note	J Shoulder Elbow Surg	2016	Low	Low
Case series	J Shoulder Elbow Surg	2018	Very Low	Low
Case series	J Orthop Surg Res	2023	Low	Low

### Preoperative simulation for corrective osteotomy of the upper limb

In 2016, we initiated the development of a 3D preoperative planning system specifically for trauma cases. The initial phase focused on creating a system for distal radius fractures, known as the distal radius fracture stage [3, 4]. This system enabled the generation of 3D models from preoperative computed tomography (CT) scans, facilitating simulations for bone fragment separation, reduction, and the selection and placement of implants. Traditionally, preoperative planning involved transcribing X-ray images onto tracing paper and making basic measurements using an image viewer. While these conventional methods are noted for their simplicity and cost-effectiveness, they fall short in allowing for the three-dimensional visualization of bone fragment manipulation and implant selection. The introduction of the 3D preoperative planning system revolutionized these processes by enabling virtual surgery, which includes detailed planning of reduction, implant selection, and verification of bone compatibility. Post-2018, the application of this system was expanded to include fractures of the elbow, carpal, and phalangeal bones. To date, it has been successfully applied in clinical settings to over 300 patients with upper extremity trauma and diseases, demonstrating significant utility and effectiveness [5–7].

At the beginning of the 3D preoperative planning system development, we speculated that this system can be applied to corrective osteotomies for malunited fractures or inherent-morphology-derived joint dysfunction. Malunited fractures are defined as synostosis of a fractured bone in a clinically abnormal form [8]. In most patients with malunited fractures, symptoms related to changes in a biomechanical state appear, while appearance is the only problem in some cases. Primary symptoms include articular pain, weakness, and functional disorder. For symptomatic malunited fractures, corrective osteotomy is necessary. The purpose of corrective osteotomy is to relieve pain and achieve functional recovery. We have been performing corrective osteotomy using 3D preoperative planning for malunions of the distal radius, distal humeral, and phalangeal fractures. The following sections introduce the specific process of 3D preoperative planning for various osteotomies.

### Distal radius malunion

Distal radius fracture is one of the most frequent fractures in human bodies [8]. The most common complication following the distal radius fracture is malunion. Its incidence is reportedly approximately 5–24% [9–12]. It is estimated that 10% of these cases require corrective osteotomy [13]. Morphological changes, such as shortening of the radius and loss of palmar tilt and radial inclination, may lead to wrist pain, a limited range of motion, and muscle weakness [14–17]. Dorsal malunion of greater than 30 degrees can lead to increased torque at the distal radioulnar joint (DRUJ) and cause functional problems with rotation of the forearm [18]. No criteria for indicating corrective osteotomy for distal radius malunion have been established, but Haase et al. defined malunion as showing (1) a radial inclination of  $\leq 10$  degrees, (2) a palmar tilt of  $\geq 20$  or  $\leq 20$  degrees, (3) an ulnar variance of  $\geq +2$  mm in comparison with the unaffected side, (4) an intra-articular step off of  $\geq 2$  mm, and (5) a radial height of  $\leq 10$  mm based on X-ray measurement of the distal radius [17]. It is necessary to evaluate these indices, the grade of disturbance, and functional requirements in individual patients when considering whether surgery should be conducted.

### Protocol

In many cases, an ideal reduction position for corrective osteotomy for the distal radius malunion can be evaluated from 3D images on injured and contralateral sides if there is no contralateral injury. For 3D preoperative planning, we generally take CT on both affected and unaffected sides, and use a reflected image on the unaffected side as a guide for the position of correction by projecting it onto the affected side. Herein, we present the concrete process of 3D preoperative planning of the distal radius. We perform CT at forearm in neutral position on unaffected- and affected-side imaging. We minimize radiation exposure by instructing patients in a sitting position to put both hands forward to place them within the extent of the CT scan. CT is performed at an approximately 13 cm extent involving the carpal bone level to the proximal wrist, with a slice width of 1 mm. Then, we import the Digital Imaging and Communications in Medicine (DICOM) data obtained from CT into the software. After segmenting the affected and unaffected sides of the radius on CT images, we prepare 3D bilateral radius models (Fig. 2). At this time, we evaluate the degree of deformity of the articular surface on the affected side by preparing a mirror image of the unaffected side and conducting alignment at a deformity-free area (Figs. 2d, 3a). Next, we prepare an image to achieve length recovery in comparison with the unaffected side and correct angular deformity. To correct angular deformities, we create an image in advance that positions a plate along the articular surface (Fig. 3b). Subsequently, we establish the osteotomy line at a location where it will not interfere with the insertion of the plate screws (Fig. 3c). An image is then created that groups the plate with the distal bone fragments post-osteotomy, and the proximal part of the plate is repositioned to the radial diaphysis to achieve the desired corrective alignment (Fig. 4). Finally, we measure the screw lengths for the proximal side of the plate, thus establish it as a preoperative plan. In the operating room, we expose a surgical field using a trans-FCR approach and perform osteotomy following the preoperative plan. Initially,

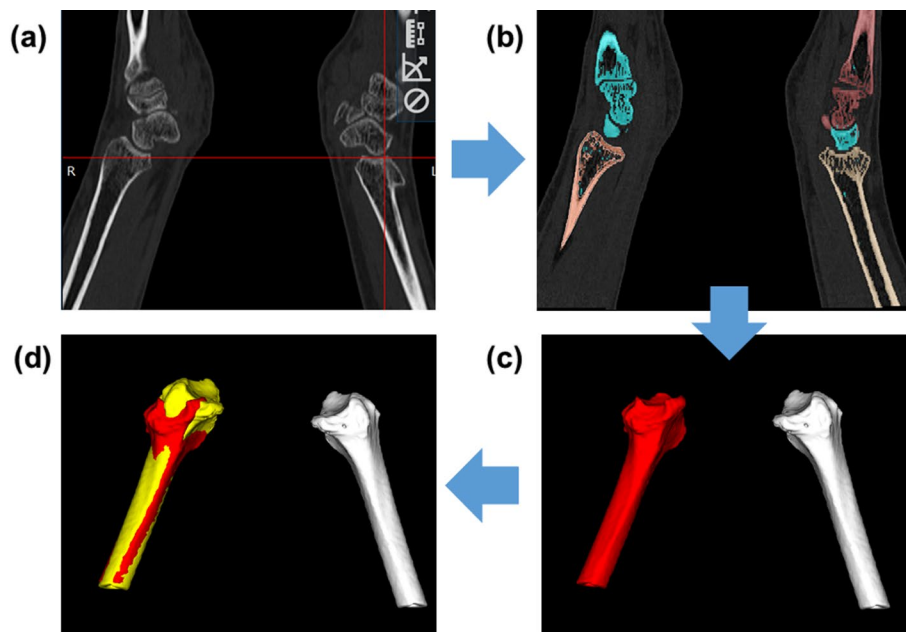


**Fig. 2** Preoperative planning process for corrective osteotomy for distal radius malunion: Step 1. **a** Import the CT data into the software. **b** Segmentations of the radius bone for both affected and unaffected side. **c** Red: Affected side 3D model, white unaffected side 3D model. **d** Yellow: mirror image of the unaffected side registered on the affected side

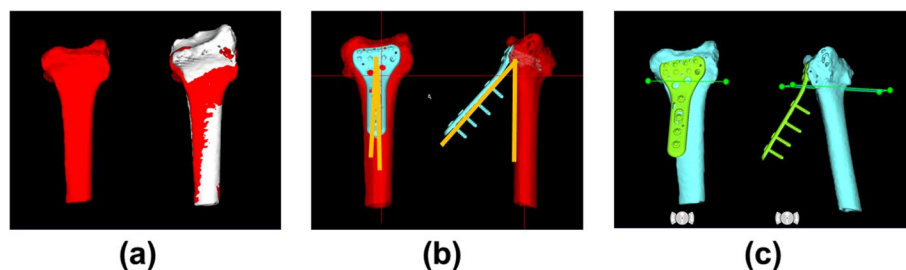


**Fig. 3** Preoperative planning process for corrective osteotomy for distal radius malunion: Step 2. **a** Red: affected side, white: unaffected side. The degree of affected-side articular surface deformity can be evaluated by aligning the two images at a deformity-free area. **b** For correction of angular deformity, an image to set a plate along the articular surface in advance is prepared. Orange lines show the correction angles. **c** Set the osteotomy line at a position that does not interfere with the plate screw insertion position

we place the distal end of the plate in parallel to the articular surface by confirming an anatomically characteristic site in the surgical field and comparing it with intraoperative fluoroscopic X-ray images. At this position, we temporary fix the plate with Kirchner wires, and create a distal-side screw hole. Subsequently, we remove the plate once while leaving the Kirchner wires as a temporary fixation (Fig. 5). After completing the osteotomy along the designated line, we reposition the plate using the wire for temporary fixation and insert distal screws, thereby ensuring that the bone fragment and plate form a unified structure. Finally, we correct the deformity by returning the proximal side of the plate to the axis of the radius bone shaft. Previously, we performed preoperative simulation in 11 patients with distal radius malunions. The

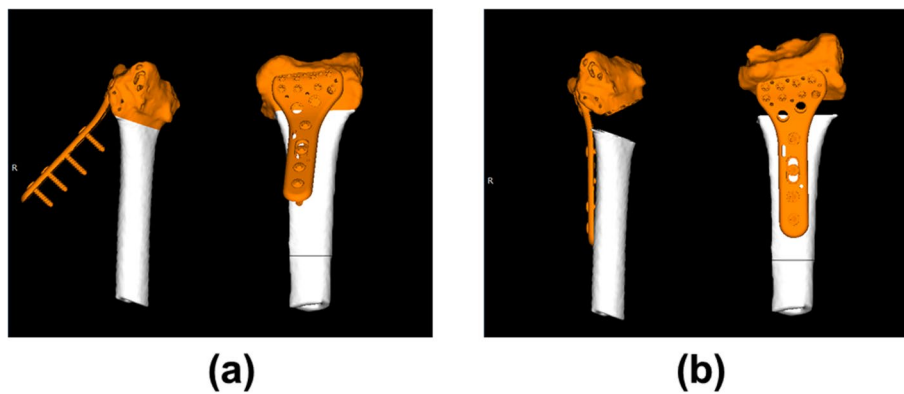


**Fig. 4** Preoperative planning process for corrective osteotomy for distal radius malunion: Step 3. **a** Group the distal bone fragment and the plate after osteotomy. **b** A correction position is obtained by returning the proximal part of the plate to the diaphysis of the radius

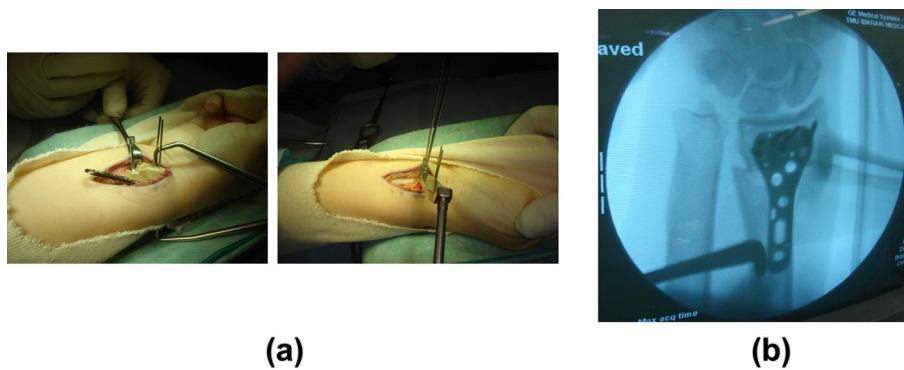


**Fig. 5** Actual surgical images of corrective osteotomy for the distal radius malunion. **a** A surgical field is exposed using a palmar approach of the wrist, and a plate is temporarily fixed based on the anatomical characteristics of the bone. The plate is removed once while leaving the Kirschner-wire for temporary fixation, and osteotomy is performed along an osteotomy line that had been planned. **b** The plate is located again via the wire for temporary fixation, and distal screws are inserted so that the bone fragment and plate may comprise a mass. Finally, a reduction position is obtained by returning the proximal side of the plate onto the axis of the radial shaft [4]

Mayo wrist score before surgery was 59 points, which was evaluated based on pain, articular angle, grip strength, and employment status, and it improved to 85 points after surgery. Based on anatomical characteristic points, we evaluated reproducibility of the procedure. It was found that reproducibility can be achieved with an error of about 2 mm based on anatomical reference points [5]. The advantages of 3D simulation include the ability to check the alignment from various directions, verify surgical procedures, and repeatedly make trials under conditions similar to actual surgery in a virtual space. These features enable orthopedic surgeons to approach surgeries with greater confidence.

**Literature review**

Recently, use of patient specific instruments (PSI) for corrective osteotomies have been becoming more common technique due to development of 3D printing technologies.

Computer-assisted corrective osteotomy has been described as a promising technique with patient specific guide. The use of custom-guided osteotomy enables accurate reduction compared with free hand technique [18–22]. Particularly, the system developed by Murase et al. [20] has been widely used in clinical settings in Japan after being included in the national insurance coverage. The advantage of PSI lies in the fact that using the cutting guide and implants obtained from preoperative planning allows for semi-automatic correction, which in turn reduces the usage of X-rays. Roner et al. introduced a patient-specific ramp-guide technique for corrective osteotomies of malunion of the distal radius, which combining navigation of plate positioning, osteotomy cutting, and reduction [23]. Using the guide, they achieved shorter duration of surgery, less residual rotational and transitional malalignment, and less misaligned screws.

Shintani et al. introduced a technique to create a prefabricated bone graft substitute to fill the bone defect during surgery of the malunited distal radius [24]. Their technique was unique in a way that they did not create patient specific cutting guides, but created a bone graft that would fit the bone defect when osteotomy and correction was done ideally. Stirling et al. reported good outcome and high level of patient satisfaction in their study which evaluated 89 patients who underwent corrective osteotomy for malunion of distal radius fractures. Ulnar styloid fracture was the only significant independent factor which worsened PRWE score. However, they did not find significant relationship between the final radiological parameters and function, neither between radiological correction and function [25]. On the other hand, Batra and Gupta reported that volar tilt as well as radial length are the most important predictor of functional recovery a year after either surgical or conservative treatment [26]. It is also reported that there is an association between ulnar variance and radial inclination and patient reported outcomes [27]. These findings indicate that achieving better reduction by means of computer-assisted surgery should lead to better clinical outcomes, however; there are not enough supportive evidence to prove this. In 2018, Bujize et al. reported in his randomized control trial a tendency of achieving better clinical results using 3D computer-assisted guidance for corrective osteotomies for extra-articular distal radius malunion [28]. These technologies seem to have the advantage of allowing surgeons to approach surgery with confidence, but more data will be needed to determine whether they improve patient clinical outcomes.

#### **Proximal phalanx/metacarpal bone malunions**

Symptomatic phalangeal and metacarpal malunions are reportedly less frequent than distal radius malunions [29]. Sagittal-plane deformity is acceptable in many cases. On the other hand, rotation deformity may cause functional disorder, such as cross fingers. There is no consensus on the permissible limit of deformity, and the indication of corrective osteotomy must be usually determined based on the grade of functional disorder [30, 31]. The purpose of corrective osteotomy is to resolve functional disorder by correcting the anatomical structure. Plain X-ray is still used as a standard method to evaluate phalangeal and metacarpal deformities. We have attempted 3D preoperative planning for these malunions. It facilitates more accurate 3D assessment of the deformities, which cannot be obtained from conventional X-ray or two-dimensional CT images.

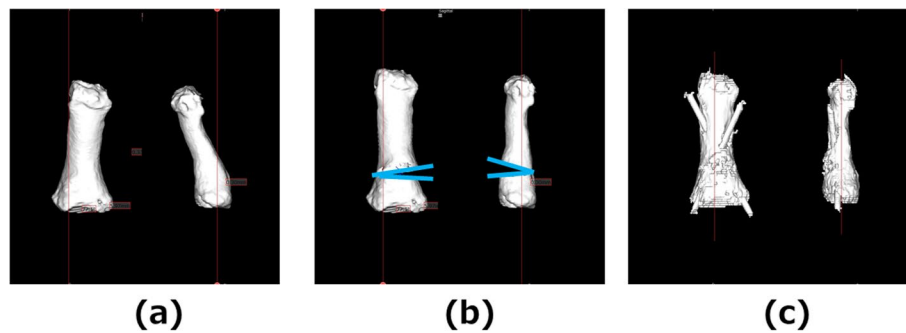


**Fig. 6** Example images of corrective osteotomy for the proximal phalanx malunion. **a** Images of proximal phalanx malunion. **b** Simulation for the corrective osteotomy. Blue lines indicate correction angle. **c** Images after the surgery

### **Protocol**

The process of preoperative planning for proximal phalanx malunion is shown in Fig. 6. As described for radius osteotomy, we use a contralateral bone model as a template for simulating deformity correction. We align a 3D model of the affected-side proximal phalanx with that of an unaffected-side mirror image at a proximal area based on the shape of the bone surface. Subsequently, we cut the bone model at the inflection point of deformity, and align the distal bone fragment with an unaffected-side mirror image. This process makes the degree of angular correction to be required clear. In the illustrated case, we observed angular deformity, however, we prepare an impression to accommodate rotation while aligning the proximal phalanx with the palmar margin of the distal condyle in patients with rotation deformity. In most phalangeal malunions, we expose the site of deformity by dividing the extensor tendon in the fiber direction through deployment from the dorsal side of the finger. Based on the distance from the articular surface measured in advance, we identify the site of osteotomy. Concerning osteotomy, we record the angle required for deformity correction on preoperative simulation (Fig. 6b), and insert Kirchner wires to the distal and proximal points of the osteotomy site as a guide for deformity correction, so that the angle can be reproduced. When a deformity is corrected, it is fixed with a 1.0–1.2-mm Kirschner wire. Previously, we performed preoperative simulation in seven patients for whom corrective phalangeal osteotomy was indicated. In all patients, bone union was achieved and resolved cross finger deformity, resulting an improvement in the finger flexion function. It is an issue for corrective osteotomy for phalangeal or metacarpal fractures that there are no versatile criteria. In the future, this involving reproducibility assessment methods should be examined.

### **Literature review**

The use of PSI has been challenged even on smaller joints; however, there have only been small number of case series reported. Singh et al. reported good radiological and functional outcome in their report of a case series of six patients [32]. They made 3D images of the injured side and mirror image of the contralateral side, and superimposed them to make plans for corrective osteotomies. In addition, patient specific guides were created

to make complexed osteotomies simple and promising on each patient. Their case series included the proximal phalanx of the ring finger, a bayonet deformity of the radius with volar and ulnar deviations, malunited Bennet fracture, malunited ulnar shaft fracture, and malunited extra-articular and intra-articular fractures of the radius. They concluded that virtual 3D analysis and surgical planning is effective to better understand the nature of the deformity, and recent advances in 3D printing technologies to create PSI can improve the short-term clinical outcomes of the malunions of small joints [32].

Kabelits et al. also reported good clinical outcomes on corrective osteotomies of small joints in their case series of ten patients [33]. The affected joints included five cases of trapeziometacarpal joints, three cases of proximal interphalangeal joints and two cases of metacarpophalangeal joints. Preoperative planning was made using 3D images of the affected side and mirror image of the unaffected side, and they created PSI for each case according to the planning. They reported excellent results on range of motion, grip strength, radiological parameters and patient-reported outcome measures. No complications were reported except four cases underwent implant removal. The effectiveness of computer-assisted corrective osteotomy of small joints including use of PSI must be confirmed under larger cohort. At the same time, application of the methods to broader injuries and dysfunctions are necessary to evaluate its usefulness.

### Utilization of the image fusion system for corrective osteotomy of the upper limb

As described in the previous sections, 3D preoperative planning has been demonstrated to be useful for the visualization of corrective osteotomy and optimization of implant selection. On the other hand, there was no method to directly compare a preoperative planning image with a fluoroscopic image, and it was impossible to evaluate the reproducibility of preoperative planning during surgery, raising an issue. We developed the image fusion system to project an image prepared for preoperative planning to an intra-operative fluoroscopic X-ray image and display it for surgical assistance (Fig. 7) [6]. Currently, navigation systems, such as 3D-multi-planar reconstruction (MPR) image-guided

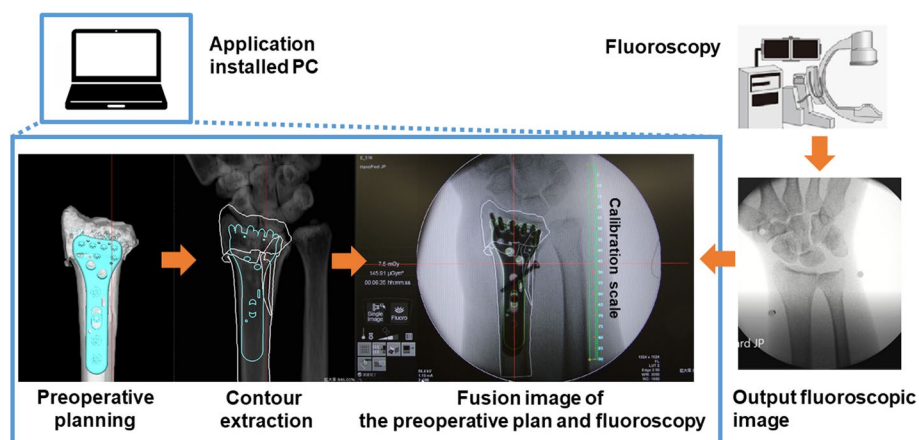


**Fig. 7** Image fusion system. Perform contour extraction processing and 2D conversion of 3D images on the application installed PC. X-ray images output from the fluoroscopy system are rendered on the Image Fusion System and compared with the contour extraction images [15]

CT-based navigation and plain X-ray image-based fluoronavigation systems, are available for osteosynthesis or corrective osteotomy. CT-based navigation involves comparison between preoperative CT and intraoperative 3D images. To achieve this, it is essential to maintain a stable intraoperative image. Consequently, using a CT-based navigation system becomes challenging for corrective osteotomy, as it involves changes in the object's position related to reduction procedures. In the fluoronavigation system, an intraoperative fluoroscopic image is imported, and the direction and depth of internal fixation material insertion are displayed on the image. However, it is impossible to obtain image of reduction by preoperative planning. Furthermore, the two systems require a high expenditure for implementation. In the image fusion system, the reproducibility of preoperative planning is simply assessed through external output of the images obtained from conventional fluoroscopy and confirmation on a personal computer (PC). For the image fusion process, we perform contour extraction processing and 2D conversion of 3D images on the application. X-ray images output from the fluoroscopy system are rendered on the image fusion system and compared with the contour extraction images. The size of the contour extraction image is adjustable (Fig. 8). Since the fluoroscopic images are output to be displayed on a PC application, the PC with the application installed is only requirement for the surgery. Contour extraction processing on 3D images and 2D-converted projection facilitated easy comparison of the simulated images with X-ray images. During surgery, one can calibrate the size of the bone based on the transverse diameter of the bone at a deformity-free site, so the surgeons can avoid changing the positional relationship between an operating table and fluoroscopy.

**Protocol**

To date, the image fusion system has been utilized in the orthopedic surgical management of various conditions, including malunited fractures of the radius and proximal phalanx bones, cubitus varus deformities, radial head dislocations secondary to acute plastic bowing of ulna, and degenerative osteoarthritis of the thumb interphalangeal (IP) joint (Fig. 9). In this chapter, we introduce an application of cubitus varus.

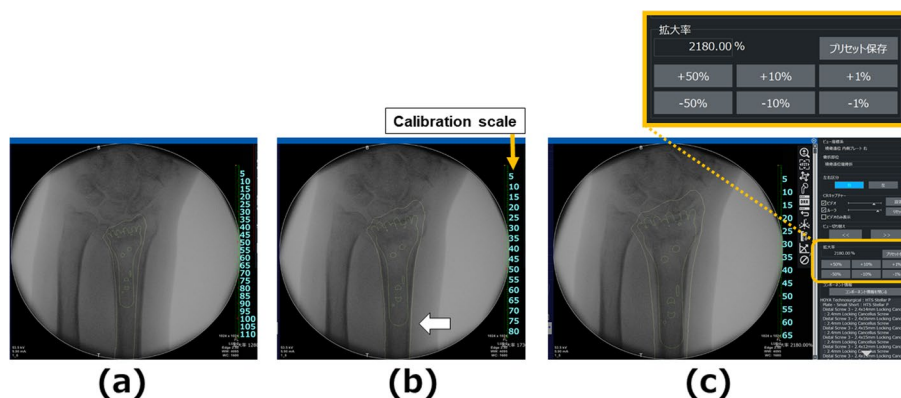


**Fig. 8** Adjustment of the contour image size. The size of the contour extraction image is adjustable. In most cases, the size of the contour extraction image is adjusted in the uninjured areas (white arrow in the figure). **a** Small contour extraction image. **b** Fitted contour extraction image. **c** Large contour extraction image. The magnification of the contour lines can be adjusted to any desired magnification with the magnification adjustment function (Yellow Square)

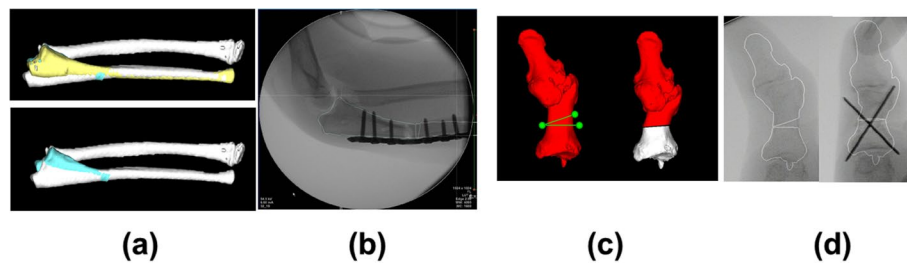


**Fig. 9** Representative cases of corrective osteotomy using Image Fusion System. **a** Radial head dislocations secondary to acute plastic bowing of ulna. White: affected side of ulna and radius, Yellow: unaffected side of ulna, Blue: after the corrective osteotomy simulation. **b** Fusion image during the surgery. **c** A case of degenerative osteoarthritis of the thumb interphalangeal (IP) joint. Green lines: osteotomy lines. **d** Fusion image during the surgery

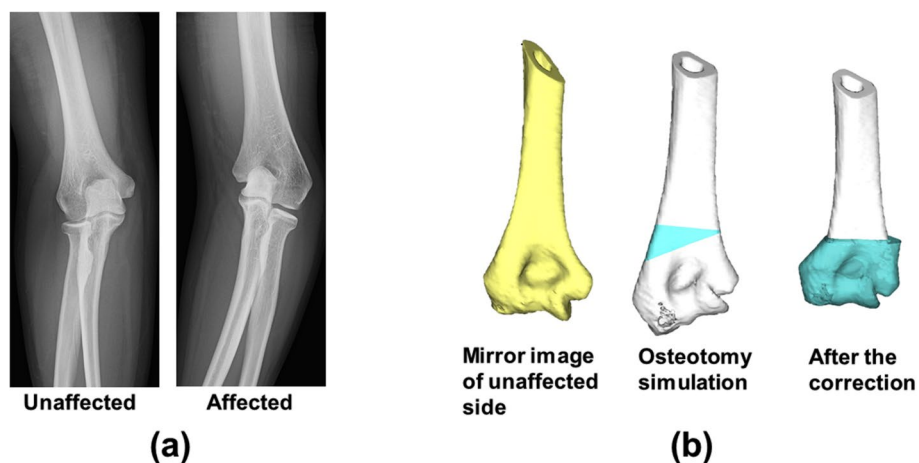


**Fig. 10** Corrective osteotomy for cubitus varus using the Image Fusion System 1. **a** X-ray images show cubitus varus on the left side elbow. **b** An image of the deformity correction position was obtained by aligning a mirror image of the unaffected-side humerus on the proximal side of the affected-side humerus. To modify the affected-side articular surface angle to the unaffected-side articular surface angle, corrective osteotomy was simulated. Yellow: mirror image of the unaffected side, White: affected side. [47]

Cubitus varus is a complication that is often observed after fracture/bone union around the elbow. It has mostly been regarded as a cosmetic problem and completely free from disturbance. However, many patients are not satisfied with the appearance of the upper extremities. Furthermore, certain proportion of patients undergo treatment for symptoms, such as chronic elbow pain and ulnar neuropathy [34–37]. Corrective osteotomy for cubitus varus is an option to correct the alignment and morbid state. To correct this complex deformity, various types of osteotomy, such as lateral closed wedge osteotomy, medial open wedge osteotomy, dome-shaped osteotomy, and step-cut osteotomy, have been proposed [38–46]. However, it is still difficult to execute an accurate preoperative plan. It is also difficult to perform accurate osteotomy according to the plan in the operating room. We performed corrective osteotomy for cubitus varus using the image fusion system [47].

In the illustrated case, we observed cubitus varus deformity related to fracture around the elbow in childhood (Fig. 10a). To improve work-related elbow pain and cosmetic aspects, the patient decided to undergo corrective osteotomy. We obtained an image

of the deformity correction position by aligning a mirror image of the unaffected-side humerus on the proximal side of the affected-side humerus. To modify the affected-side articular surface angle to the unaffected-side articular surface angle, we simulated corrective osteotomy (Fig. 10b). On simulation, we chose closed wedge osteotomy at the inflection point of deformity. We prepared an image to achieve approximately 30-degree correction of the varus angle and approximately 15-degree correction of the forward tilt angle by osteotomy in conformity with the unaffected-side articular surface. We prepared a 3D image in which an osteotomy line was established for the image fusion system, as well as a 3D image of the state after reduction, and conducted contour extraction processing at a position where an osteotomy line seemed to be one plane (Fig. 11). We performed surgery while projecting a contour extraction processing image that had been stored onto an intraoperative fluoroscopic image after external output. For surgery, we exposed the site of osteotomy using a posterior elbow approach. Along the osteotomy line projected onto a fluoroscopic image, we inserted two Kirshner wires and performed osteotomy. When obtaining a correction position, we projected a contour image of the post-reduction model, and conducted reduction to match the articular surface and the projected contour. As a result, the articular surface tilt was improved by 23 degrees, and the forward tilt angle by 16 degrees.

#### Literature review

Corrective osteotomy for cubitus varus deformity in adults induces many complications, such as a limited range of motion and delayed bone union [48]. It is necessary to achieve a normal elbow-like morphology by reduction and perform accurate osteotomy with no gap on the osteotomy surface. The image fusion system is a new approach for corrective osteotomy in which 3D simulation is combined with fluoroscopic images. This system facilitates preoperative planning and direct comparison with fluoroscopic images. With visual support for the surgical process, orthopedic surgeons can perform corrective osteotomy with confidence.

A study reported the use of a PSI for corrective osteotomy for cubitus varus deformity [48]. PSI facilitates accurate, simple three-dimensional corrective osteotomy, and its usefulness and reproducibility are suggested. As a demerit of PSI, 8–12 weeks are required

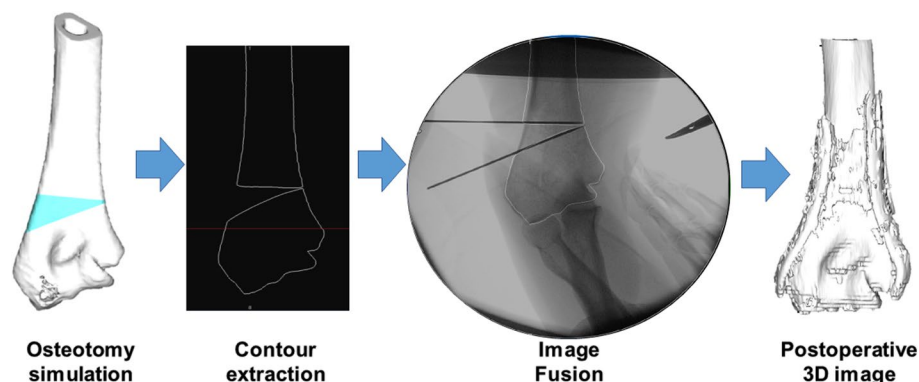


**Fig. 11** Corrective osteotomy for cubitus varus using the Image Fusion System 2. A contour extraction processing was conducted. Along the osteotomy line projected onto a fluoroscopic X-ray image, Kirshner wires were inserted. Along the Kirshner wire, osteotomy was performed [47]

for the preparation of the relevant equipment. Furthermore, the cost of devices related to surgery is about 3.86-times higher than that of conventional devices. When the image fusion system is used, the osteotomy site on preoperative planning is projected onto a fluoroscopic image during surgery, facilitating accurate osteotomy through the identification of the osteotomy site. As a merit of the image fusion system, orthopedic surgeons responsible for surgery can execute a preoperative plan by themselves, and take it to the operating room in a short time. They can understand an optimal bone shape for the patient in advance through simulation in a virtual space. As another merit, the cost of this system is lower than that of PSI. As a ready-made implant is placed in an optimal position, the cost of original implant preparation is not required. On the other hand, currently, preoperative simulation has no function to curve a ready-made implant in accordance with the patient's bone shape; therefore, on simulation, it is necessary to place a ready-made implant, so that it may be matched to the state of reduction. In addition, intraoperative fluoroscopic images are two-dimensional, and there is a difference in the magnification rate between areas adjacent to and distal from an irradiated site due to a lack of depth information; the osteotomy position may be inaccurately visualized. Considering these points, further improvements are necessary for the reproduction of preoperative planning with the image fusion system. Currently, to overcome these issues, techniques to rearrange intraoperative X-ray images and estimate the 3D position of X-ray images are being developed [49, 50]. In the future, these techniques may be implemented on the image fusion system.

It seems that it is more common to use PSI for corrective osteotomies cubitus varus deformity of the elbow than for distal radius fractures. There are numbers of recent articles that describe the usefulness of PSI [51–57]. The techniques introduced in the articles are similar that they create mirror image of 3D model of the humerus using CT data of the contralateral side, then virtually simulate corrective osteotomies to fit the contralateral side. PSI are made to adequately execute the osteotomy using the 3D printers. Even an preoperative simulated surgery using 3D printed bone model, not virtual, is also reported effective in conducting surgery as planned [58]. These reports have in common that the operation time and blood loss would be decreased using the technique; however, there are not enough evidence to show that the technique is effective to achieve better clinical outcomes.

### **Cons and pros of the computer-assisted surgery and future perspectives**

As we discussed above, three-dimensional, computer-assisted preoperative planning provide surgeons clearer vision of surgical procedures. In addition, use of PSI makes complexed corrective osteotomy relatively a simple procedure with promising deformity correction. These are great advantages of the procedure.

On the other hand, as a disadvantage of computer assisted surgery, it is reported that the design of the patient specific guide is challenging [23], and simulation of surgery is time-consuming, which may take 2–4 h per case. In general, in case of malunions or deformities, surgery would not be scheduled urgently. Therefore, the advantage of making precise 3D preoperative planning and creation of PSI may overwhelm the caused delay. Furthermore, every computer-assisted system need additional cost, even our novel intraoperative reference system, the image fusion system. When surgeon use 3D

simulation system and create PSI, the additional cost would be up to 4300 USD per case [23, 52, 59]. We must consider cost–benefit of the system when applying it to actual practice. In the future, a low-cost system that is easier to use should be established by introducing new techniques.

For the future perspectives, advancements in artificial intelligence (AI) are expected to play a significant role in the computer-assisted surgery [60–62]. The integration of AI offers great potential for supporting decision-making during operations and enabling greater automation, which can enhance success rates and alleviate the physical and cognitive burden on surgeons. In addition, robotic technology will continue to evolve, allowing for more precise and delicate procedures [63–65]. This progress will also lead to advancements in remote and automated surgeries, expanding the scope of surgical interventions. Moreover, computer-assisted surgery will facilitate the realization of personalized medicine. These technologies will enable individualized treatments by considering each patient's unique anatomy and medical conditions, leading to more accurate and effective outcomes. Furthermore, with the rapid development of high-speed communication technologies, remote surgeries will become increasingly feasible [66, 67]. Specialists will be able to perform surgeries from distant locations, improving access to advanced healthcare and providing patients with world-class expertise, regardless of their geographical location.

### **Limitations**

While this review provides an in-depth analysis of the current advancements in three-dimensional preoperative planning and computer-assisted surgery for corrective osteotomy, several limitations must be acknowledged. First, many of the studies reviewed in this study had small sample sizes, limiting the generalizability of the findings. Small cohorts may not capture the full spectrum of clinical outcomes or complications, making it challenging to draw definitive conclusions about the widespread efficacy of these technologies. Second, the reviewed literatures include a wide range of study designs, from case series and retrospective studies to small prospective trials. This heterogeneity in methodology limits the ability to directly compare results and synthesize clear, evidence-based conclusions. Third, the outcomes reported across the reviewed studies vary significantly, with some focusing on radiological parameters, while others emphasize clinical outcomes, such as pain reduction or functional improvement. The lack of standardized outcome measures makes it difficult to assess the true impact of these technologies on patient care and recovery. Fourth, while the technologies reviewed have shown promise in improving surgical precision, their costs remain a significant barrier to widespread adoption, particularly in low-resource settings. To improve the cost-effectiveness, we need to consider streamline production with affordable 3D printing, adopt open-source planning software, and implement modular systems for scalable use. In addition, the implementation of 3D preoperative planning and PSI requires a steep learning curve and technical expertise. Surgeons need specialized training to effectively use these systems, which may delay their integration into routine practice. In our experience, the time for the 3D preoperative planning reduced 78% (originally took about 90 min, and after get familiar with the software, it took less than 20 min). Workshops and other opportunities to become familiar with these technologies should be considered (Fig. 12). Fifth,

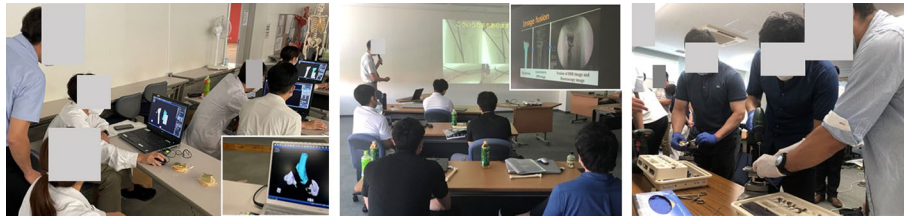


**Fig. 12** Workshops for the 3D preoperative planning

regarding the image fusion system, our primary focus has been on single-bone corrections to validate its feasibility and accuracy. Although we have not yet applied the system to simultaneous corrections of multiple bones, such as the radius and ulna, we recognize its potential for these applications and plan to address this in future studies. In addition, the system currently does not account for soft tissue impairment, emphasizing the need to integrate soft tissue considerations in future research. Finally, many studies focused on short-term clinical outcomes, such as the accuracy of osteotomy and immediate postoperative recovery. However, there is a lack of long-term data on patient-reported outcomes, functional recovery, and the durability of the corrections achieved using these technologies. Further research is needed to evaluate the long-term benefits and potential complications of 3D preoperative planning and computer-assisted surgery.

## Conclusions

This article highlights the benefits of computer-assisted techniques, including 3D preoperative planning and the image fusion system, for corrective osteotomy of the upper limb. While their impact on clinical outcomes is not yet definitive, these tools enhance surgical precision, improve preoperative visualization, and provide greater confidence in complex procedures. These innovations offer significant potential for improving surgical accuracy and patient satisfaction, despite current barriers, such as cost and technical complexity. Future advancements in artificial intelligence and robotics are expected to further enhance these systems, enabling broader applications and personalized surgical interventions. Continued research is essential to validate their long-term clinical impact and optimize their accessibility.

## Abbreviations

3D	Three-dimensional
CT	Computed tomography
PSI	Patient-specific instruments
DRUJ	Distal radioulnar joint
DICOM	Digital imaging and communications in medicine
PC	Personal computer
MRI	Magnetic resonance imaging
X-ray	X-radiation
MPR	Multi-planar reconstruction
FCR	Flexor carpi radialis
AO	Arbeitsgemeinschaft für Osteosynthesefragen (Association for the Study of Internal Fixation)
ICC	Intra-class correlation coefficients
PRWE	Patient-rated wrist evaluation
IP	Interphalangeal
USD	United States Dollar
AI	Artificial intelligence

### Author contributions

YY: research design, acquisition and analysis of data, and wrote the manuscript, SK: acquisition and analysis of data and revise the manuscript, AI: acquisition and analysis of data and revise the manuscript, YY: acquisition and analysis of data and revise the manuscript, TN: acquisition and analysis of data and wrote the manuscript, JM: research design, interpretation of results, and wrote the manuscript, TO: acquisition and analysis of data and wrote the manuscript. All authors were fully involved in the study and approved the final version of this manuscript.

### Funding

This study was supported by a Grant-in-Aid for Scientific Research (23K08618), the General Insurance Association of Japan, and Terumo Life Science Foundation. These funds were not involved in data collection, data analysis, or the preparation or editing of the manuscript.

### Availability of data and materials

No data sets were generated or analysed during the current study.

### Declarations

#### Ethics approval and consent to participate

This study was performed in line with the principles of the Declaration of Helsinki. This study protocol was approved by the Institutional Review Board of Tokyo Medical University Ibaraki Medical Center.

#### Consent for publication

Written consent for publication was obtained from all study participants.

#### Competing interests

The authors declare no competing interests.

Received: 16 July 2024 Accepted: 6 January 2025

Published online: 15 January 2025

### References

1. Page MJ, McKenzie JE, Bossuyt PM, Boutron I, Hoffmann TC, Mulrow CD, Shamseer L, Tetzlaff JM, Akl EA, Brennan SE, Chou R, Glanville J, Grimshaw JM, Hróbjartsson A, Lalu MM, Li T, Loder EW, Mayo-Wilson E, McDonald S, McGuinness LA, Stewart LA, Thomas J, Tricco AC, Welch VA, Whiting P, Moher D. The PRISMA 2020 statement: an updated guideline for reporting systematic reviews. *BMJ*. 2021;372:n71.
2. Guyatt GH, Oxman AD, Schünemann HJ, Tugwell P, Knottnerus A. GRADE guidelines: a new series of articles in the *Journal of Clinical Epidemiology*. *J Clin Epidemiol*. 2011;64(4):380–2.
3. Yoshii Y, Kusakabe T, Akita K, Tung WL, Ishii T. Reproducibility of three-dimensional digital preoperative planning for the osteosynthesis of distal radius fractures. *J Orthop Res*. 2017;35:2646–51.
4. Yoshii Y. Preoperative simulation and image fusion system for the corrective osteotomy of upper extremity. *J Tokyo Med Univ*. 2024;82:131–41.
5. Yoshii Y, Ogawa T, Hara Y, Totoki Y, Ishii T. An image fusion system for corrective osteotomy of distal radius malunion. *Biomed Eng Online*. 2021;20:66.
6. Yoshii Y, Totoki Y, Sashida S, Sakai S, Ishii T. Utility of an image fusion system for 3D preoperative planning and fluoroscopy in the osteosynthesis of distal radius fractures. *J Orthop Surg Res*. 2019;14:342.
7. Kohyama S, Yoshii Y, Ikumi A, Ogawa T, Ishii T. Is a novel fluoroscopic intraoperative reference system superior to conventional management for distal radius fracture reduction? A propensity-matched comparative study. *Clin Orthop Relat Res*. 2024;482:526–33.
8. Sarmiento A, Sobol PA, Hoy ALS, Ross SD, Racette WL, Tarr RR. Prefabricated functional braces for the treatment of fractures of the tibial diaphysis. *J Bone Joint Surg Am*. 1984;66:1328–39.
9. Cooney WP, Dobyns JH, Linscheid RL. Complications of Colles' fractures. *J Bone Joint Surg Am*. 1980;62:613–9.
10. Mulders MAM, d'Ailly PN, Cleffken BI, Schep NWL. Corrective osteotomy is an effective method of treating distal radius malunions with good long-term functional results. *Injury*. 2017;48:731–7.
11. Viegas SF. A new modification of corrective osteotomy for treatment of distal radius malunion. *Tech Hand Upper Extremity Surg*. 2006;10:224–30.
12. Katt B, Seigerman D, Lutsky K, Beredjiklian P. Distal radius malunion. *J Hand Surg Am*. 2020;45:433–42.
13. Wilcke MKT, Hammarberg H, Adolphson PY. Epidemiology and changed surgical treatment methods for fractures of the distal radius: a Registry analysis of 42583 patients in Stockholm County, Sweden, 2004–2010. *Acta Orthop*. 2013;84(3):292–6.
14. Bushnell BD, Bynum DK. Malunion of the distal radius. *J Am Acad Orthop Surg*. 2007;15:27–40.
15. Graham TJ. Surgical correction of malunited fractures of the distal radius. *J Am Acad Orthop Surg*. 1997;5:270–81.
16. Park MJ, Cooney WP, Hahn ME, Looi KP, An KN. The effects of dorsally angulated distal radius fractures on carpal kinematics. *J Hand Surg Am*. 2002;27:223–32.
17. Haase SC, Chang KC. Management of malunions of the distal radius. *Hand Clin*. 2012;28:207–16.
18. Prommersgerger KJ, Schoonhoven JV, Lanz UB. Outcome after corrective osteotomy for malunited fractures of the distal end of the radius. *J Hand Surg Br*. 2002;27(1):55–60.
19. Schweizer A, Fürnstahl P, Nagy L. Three-dimensional correction of distal radius intra-articular malunions using patient-specific drill guides. *J Hand Surg Am*. 2013;38(12):2339–47.

20. Murase T, Oka K, Moritomo H, Goto A, Yoshikawa H, Sugamoto K. Three-dimensional corrective osteotomy of malunited fractures of the upper extremity with use of a computer simulation system. *J Bone Joint Surg Am*. 2008;90(11):2375–89.
21. Vlachopoulos L, Schweizer A, Graf M, Nagy L, Fűrnstahl P. Three-dimensional postoperative accuracy of extra-articular forearm osteotomies using CT-scan based patient-specific surgical guides. *BMC Musculoskelet Disord*. 2015;16:336.
22. Schweizer A, Mauler F, Vlachopoulos L, Nagy L, Fűrnstahl P. Computer-assisted 3-dimensional reconstructions of scaphoid fractures and nonunions with and without the use of patient-specific guides: early clinical outcomes and postoperative assessments of reconstruction accuracy. *J Hand Surg Am*. 2016;41(1):59–69.
23. Roner S, Carillo F, Vlachopoulos L, Schweizer A, Nagy L, Fűrnstahl P. Improving accuracy of opening-wedge osteotomies of distal radius using a patient-specific ramp-guide technique. *BMC Musculoskelet Disord*. 2018;19:374.
24. Shintani K, Kazuki K, Yobeda M, Uemura T, Okada M, Takamatsu K, Nakamura H. Computer-assisted three-dimensional corrective osteotomy for malunited fractures of the distal radius using prefabricated bone graft substitute. *J Hand Surg Asian Pac*. 2018;23(4):479–86.
25. Stirling PHC, Oliver WM, Tan HL, Brown IDM, Oliver CW, McQueen MM, Molyneux SG, Duckworth AD. Patient-reported outcomes after corrective osteotomy for a symptomatic malunion of the distal radius. *Bone Joint J*. 2020;102-B(11):1542–8.
26. Batra S, Gupta A. The effect of fracture-related factors on the functional outcome at 1 year in distal radius fractures. *Injury*. 2002;33(6):499–502.
27. Ali M, Brogen E, Wagner P, Atroshi I. Association between distal radial fracture malunion and patient-reported activity limitations: a log-term follow-up. *J Bone Joint Surg Am*. 2018;100:633–9.
28. Bujize GA, Leong NL, Stockmans F, Axelsson P, Moreno R, Sørensen AI, Jupiter JB. Three-dimensional compared with two-dimensional preoperative planning of corrective osteotomy for extra-articular distal radial malunion: a multi-center randomized controlled trial. *J Bone Joint Surg Am*. 2018;100:1191–202.
29. Hirsiger S, Schweizer A, Miyake J, Nagy L, Fűrnstahl P. Corrective osteotomies of phalangeal and metacarpal malunions using patient-specific guides: CT-based evaluation of the reduction accuracy. *Hand*. 2018;13:627–36.
30. Buchler U, Gupta A, Ruf S. Corrective osteotomy for post-traumatic malunion of the phalanges in the hand. *J Hand Surg Br*. 1996;21:33–42.
31. Gollamudi S, Jones WA. Corrective osteotomy of malunited fractures of phalanges and metacarpals. *J Hand Surg Br*. 2000;25:439–41.
32. Singh S, Andrinuc O, Kaiser P, Jud L, Nagy L, Schweizer A. Recent advances in the surgical treatment of malunions in hand and forearm using three-dimensional planning and patient-specific instruments. *Hand Surg Rehabil*. 2020;39:352–62.
33. Kabelitz M, Furrer PR, Hodel S, Canonica S, Schweizer A. 3D planning and patient specific instrumentation for intraarticular corrective osteotomy of trapeziometacarpal-, metacarpal and finger joints. *BMC Musculoskelet Disord*. 2022;23:965.
34. Abe M, Ishizu T, Morikawa J. Posterolateral rotatory instability of the elbow after posttraumatic cubitus varus. *J Shoulder Elb Surg*. 1997;6:405–9.
35. Mitsunari A, Muneshige H, Ikuta Y, Murakami T. Internal rotation deformity and tardy ulnar nerve palsy after supracondylar humeral fracture. *J Shoulder Elb Surg*. 1995;4:23–9.
36. O'Driscoll SW, Spinner RJ, McKee MD, Kibler WB, Hastings H, Morrey BF, et al. Tardy posterolateral rotatory instability of the elbow due to cubitus varus. *J Bone Joint Surg Am*. 2001;83:1358–69.
37. Spinner RJ, Goldner RD. Snapping of the medial head of the triceps and recurrent dislocation of the ulnar nerve. Anatomical and dynamic factors. *J Bone Joint Surg Am*. 1998;80:239–427.
38. Davids JR, Lamoreaux DC, Brooker RC, Tanner SL, Westberry DE. Translation step-cut osteotomy for the treatment of posttraumatic cubitus varus. *J Pediatr Orthop*. 2011;31:353–65.
39. DeRosa GP, Graziano GP. A new osteotomy for cubitus varus. *Clin Orthop Relat Res*. 1988;236:160–5.
40. French PR. Varus deformity of the elbow following supracondylar fractures of the humerus in children. *Lancet*. 1959;2:439–41.
41. Kim HS, Jahng JS, Han DY, Park HW, Kang HJ, Chun CH. Modified step-cut osteotomy of the humerus. *J Pediatr Orthop B*. 1998;7:162–6.
42. Laupattarakasem W, Mahaisavariya B, Kowsuwon W, Saengnipanthkul S. Pentalateral osteotomy for cubitus varus. *J Bone Joint Surg Br*. 1989;71:667–70.
43. Matsushita T, Nagano A. Arc osteotomy of the humerus to correct cubitus varus. *Clin Orthop*. 1997;336:111–5.
44. Tien YC, Chih HW, Lin GT, Lin SY. Dome corrective osteotomy for cubitus varus deformity. *Clin Orthop Relat Res*. 2000;380:158–66.
45. Uchida Y, Ogata K, Sugioka Y. A new three-dimensional osteotomy for cubitus varus deformity after supracondylar fracture of the humerus in children. *J Pediatr Orthop*. 1991;11:327–31.
46. Kim JR, Moon YJ, Wang SI. Translation step-cut osteotomy for posttraumatic cubitus varus in adults: a retrospective study. *BMC Musculoskelet Disord*. 2020;21:820.
47. Morita J, Yoshii Y, Nakatani T, Ogawa T, Mishima H, Ishii T. Corrective osteotomy for cubitus varus using the Image Fusion System. *JOS Case Rep*. 2024;3:151–4.
48. Takeyasu Y, Oka K, Miyake J, Kataoka T, Moritomo H, Murase T. Preoperative, computer simulation-based, three-dimensional corrective osteotomy for cubitus varus deformity with use of a custom-designed surgical device. *J Bone Joint Surg Am*. 2013;95:e173.
49. Shrestha P, Xie C, Shishido H, Yoshii Y, Kitahara I. 3D Reconstruction of Wrist Bones from C-Arm Fluoroscopy Using Planar Markers. *Diagnostics*. 2023;13:330.
50. Yoshii Y, Iwahashi Y, Sashida S, Shrestha P, Shishido H, Kitahara I, Ishii T. An experimental study of a 3D bone position estimation system based on fluoroscopic images. *Diagnostics*. 2022;12:2237.
51. Barbier NF, Wouters SD, Traore SY, Duy KT, Docquier PL. Patient specific instrumentation for corrective osteotomy in case of posttraumatic cubitus varus in children. *Acta Orthop Belg*. 2019;85:297–304.

52. Bauer DE, Zimmermann S, Aichmair A, Hingsammer A, Schweizer A, Nagy L, Fürnstahl P. Conventional versus computer-assisted corrective osteotomy of the forearm: a retrospective analysis of 56 consecutive cases. *J Hand Surg Am.* 2017;42:447–55.
53. Zhang YW, Xiao X, Gao WC, Xiao Y, Zhang SL, Ni WY, Deng L. Efficacy evaluation of three-dimensional printing assisted osteotomy guide plate in accurate osteotomy of adolescent cubitus varus deformity. *J Orthop Surg Res.* 2019;14:353.
54. Li J, Wang J, Rai S, Ze RH, Hong P, Wang SY, Tang X. 3D-printed model and osteotomy template technique compared with conventional closing-wedge osteotomy in cubitus varus deformity. *Sci Rep.* 2022;12:6762.
55. Hu X, Zhong M, Lou Y, Xu P, Jiang B, Mao F, Chen D, Zheng P. Clinical application of individualized 3D- printed navigation template to children with cubitus varus deformity. *J Orthop Surg Res.* 2020;15:111.
56. Vlachopoulos L, Schweizer A, Meyer DC, Gerber C, Fürnstahl P. Three-dimensional corrective osteotomies of complex malunited humeral fractures using patient-specific guides. *J Shoulder Elbow Surg.* 2016;25:2040–7.
57. Oura K, Shigi A, Oka K, Tanaka H, Murase T. Corrective osteotomy for hyperextended elbow with limited flexion due to supracondylar fracture malunion. *J Shoulder Elbow Surg.* 2018;27:1357–65.
58. Xue KX, Zheng XG, Qiao C, Fang JH. Preoperative simulated surgery on 3D model assists osteotomy feasibility verification and surgical guidance for patients with cubitus valgus/varus deformity: a retrospective observational study. *J Orthop Surg Res.* 2023;18(1):470.
59. Byrne AM, Impelmans B, Bertrand V, Haver AV, Verstrecken F. Corrective osteotomy for malunited diaphyseal forearm fractures using preoperative 3-dimensional planning and patient-specific surgical guides and implants. *J Hand Surg.* 2017;42(10):836.
60. Lambrechts A, Wirix-Speetjens R, Maes F, Van Huffel S. Artificial intelligence based patient-specific preoperative planning algorithm for total knee arthroplasty. *Front Robot AI.* 2022;9:840282.
61. Anwar A, Zhang Y, Zhang Z, Li J. Artificial intelligence technology improves the accuracy of preoperative planning in primary total hip arthroplasty. *Asian J Surg.* 2024;47(7):2999–3006.
62. Takeuchi M, Kitagawa Y. Artificial intelligence and surgery. *Ann Gastroenterol Surg.* 2023;8(1):4–5.
63. Suarez-Ahedo C, Lopez-Reyes A, Martinez-Armenta C, Martinez-Gomez LE, Martinez-Nava GA, Pineda C, Vanegas-Contla DR, Domb B. Revolutionizing orthopedics: a comprehensive review of robot-assisted surgery, clinical outcomes, and the future of patient care. *J Robot Surg.* 2023;17(6):2575–81.
64. Li T, Badre A, Alambeigi F, Tavakoli M. Robotic systems and navigation techniques in orthopedics: a historical review. *Appl Sci.* 2023;13(17):9768.
65. Mamdouhi T, Wang V, Echevarria AC, Katz A, Morris M, Zavurov G, Verma R. A comprehensive review of the historical description of spine surgery and its evolution. *Cureus.* 2024;16(2):e54461.
66. Merle G, Miclau T, Parent-Harvey A, Harvey EJ. Sensor technology usage in orthopedic trauma. *Injury.* 2022;53(Suppl 3):S59–63.
67. Grandizio LC, Foster BK, Klena JC. Telemedicine in hand and upper-extremity surgery. *J Hand Surg Am.* 2020;45(3):239–42.

### **Publisher's Note**

Springer Nature remains neutral with regard to jurisdictional claims in published maps and institutional affiliations.